Computational Materials Science 50 (2010) 790–795

Contents lists available at ScienceDirect

Computational Materials Science

journal homepage: www.elsevier.com/locate/commatsci

Molecular dynamics study on oscillation dynamics of a C_{60} fullerene encapsulated in a vibrating carbon-nanotube-resonator

Jeong Won Kang [a], Ho Jung Hwang [b,*]

[a] Department of Computer Engineering, Chungju National University, Chungju 380-702, Republic of Korea
[b] School of Electrical and Electronic Engineering, Chung-Ang University, Seoul 156-756, Republic of Korea

ARTICLE INFO

Article history:
Received 14 September 2010
Accepted 11 October 2010
Available online 30 October 2010

Keywords:
Nanotube oscillator
Carbon-nanotube
C_{60} Fullerene
Molecular dynamics

ABSTRACT

We investigated the oscillation dynamics of a C_{60} fullerene encapsulated in a single-walled carbon-nanotube-resonator via classical molecular dynamics simulations. The C_{60} fullerene positions in a single-walled carbon-nanotube-resonator could be controlled by vibrating the resonator. The C_{60}-fullerene's oscillations along the tube axis in a vibrating carbon-nanotube-resonator were originated by centrifugal forces exerted at the central position of the vibrating carbon-nanotube, and thus property was very different from its oscillation due to van der Waals forces in the fixed carbon-nanotube. These properties suggest that a carbon-nanotube-resonator encapsulating a C_{60} fullerene has a potential application for programmable multiple-position devices controlled by the resonance frequency.

1. Introduction

Nano-electromechanical resonators have been considered for various applications such as precision mass sensing, electronic devices, signal processing and medicines [1]. Carbon-nanotubes (CNTs) [2] have been investigated by some researchers for their potential applications as resonators [3] and oscillators [4], resulting in gigahertz resonators that can be applied to nanoscale sensors, actuators, resonators, injectors, motors, engines, filters, memory, and switching devices [5].

The C_{60} fullerene is a spherical carbon cage of atoms that are held together to form a closed-packed structure [6]. CNTs encapsulating fullerenes, called nanopeapods, have been synthesized and their properties have been widely investigated [7]. After investigating the fullerene intercalates inside carbon-nanotubes as a fullerene shuttle memory device via experiments and molecular dynamics simulations [8], the authors of this paper have investigated $K@C_{60}@C_{640}$ as a fullerene shuttle memory device [9], the three-terminal transistor [10], and $F@C_{60}$ encapsulated in a C_{640} as an electro-fluidic shuttle memory device. [11] Since the determination of the band gap for carbon nanopeapods encapsulating fullerene molecules [12], the present authors proposed various nanomemory devices based on nanopeapods [13]. A more comprehensive study on the influence of van der Waals interactions between the embedded fullerenes and the nanotube for the nanopeapods geometric configuration has also been proposed [14]. Fullerenes may enter into boron-nitride nanotubes easier than carbon-nanotubes, and a nanomemory device based on boron-nitride nanopeapods has been investigated [15,16]. The present authors further made a comparison between carbon and boron-nitride nanopeapods of the fullerene shuttle memory device using atomistic simulations [17], and a summary of the above nanomaterial based memory device can be found in [18].

In this paper, we investigate an (10,10) CNT encapsulating a C_{60} fullerene (C_{60}@CNT) resonator via classical molecular dynamics (MD) simulations, which have widely been used to study and predict the dynamics properties of nanoscale materials such as nanotubes, nanowires, and nanoparticles [19–24]. The vibrations of the encapsulated C_{60} fullerene during the vibrating single-walled (10,10) CNT resonator were analyzed by the data obtained from the MD simulations. Specially, we focused the position change along the tube axis, and we then found that the encapsulated C_{60} fullerene could be oscillated along the tube axis, and its oscillation was damped to approach the center of the CNT resonator due to the acceleration force exerted by the vibrating CNT. Due to the van der Waals interaction force as suction force at both edges, which has been extensively investigated, the acceleration-force-induced C_{60}-fullerene's oscillation inside CNT addressed in this work is very different from its oscillation [25–31]. We also investigated the vibration frequency raised by the position change along the tube axis. These properties suggest that a CNT resonator encapsulating a C_{60} fullerene has a potential application in a programmable position device as a fullerene-shuttle-memory [8,9].

* Corresponding author. Tel.: +82 2 820 5296; fax: +82 2 812 5318.
E-mail address: hjhwang@cau.ac.kr (H.J. Hwang).

0927-0256/$ - see front matter © 2010 Elsevier B.V. All rights reserved.
doi:10.1016/j.commatsci.2010.10.014

2. Simulation methods

To study the dynamics of a C_{60} fullerene encapsulating a vibrating CNT-resonator, we considered a (10,10) single-walled CNT encapsulating a C_{60} fullerene as shown in Fig. 1a. A (10,10) CNT with a length of about 13 nm was used as shown in Fig. 1, and both clamped boundaries were opened. The initial structures were relaxed by simulated annealing simulations; then, the C_{60} fullerene in the (5,5) CNT was optimized.

The carbon–carbon interactions were based on the Tersoff–Brenner potential function [32–34] that has been widely applied to carbon systems. The interactions between C_{60} and CNT were characterized using the Lennard–Jones 12–6 (LJ12–6) potential based on the parameters of Ulbricht et al. [35]. The respective parameters that we used for the LJ12–6 potential were $\varepsilon_{carbon} = 2.4038 \times 10^{-3}$ eV and $\sigma_{carbon} = 3.37$ Å. The cutoff distance of the LJ12–6 potential was 10 Å.

We performed the MD simulations based on the MD methods from our previous studies [36–38]. The MD code uses the velocity Verlet algorithm and neighbor lists to improve the computing performance. The MD time step (Δt) was 5×10^{-4} ps. The temperature for all MD simulations was set to 1 K, and the total MD time was set to 1 ns. Both ends of the (10,10) CNT were fixed, and MD simulations were created for the other atoms. To simulate the oscillations of the CNT resonator, an external force field with the fundamental resonance frequency was applied in the transverse direction of the tube axis in order to obtain the vibrating CNT. The vibration frequencies of the C_{60} fullerene were obtained form the results using the fast Fourier transform method.

3. Results and discussion

First, we performed a MD simulation during 1 ns under the condition of an external force applied to the transverse of the tube axis during the initial 0.01 ns, and thus the fundamental resonance frequency (f_0) was calculated and several atomic configurations were obtained from the data of the MD simulation for the displacement (Y_{disp}) of CNT. Second, via a steepest descent method, we optimized the deformed CNTs corresponding to Y_{disp} using several atomic configurations obtained from the MD simulation, and we then structurally re-optimized C_{60}@CNTs under the position variations (P_{C60}) of the C_{60} fullerene, and we finally obtained the vdW energies (U_{vdW}) as functions of the C_{60}'s position and Y_{disp}.

Fig. 1a shows six atomic configurations corresponding to six P_{C60} values for $Y_{disp} = 1.3$ nm. Fig. 1b shows a three-dimensional plot of the U_{vdW} variations as functions of P_{C60} and Y_{disp}, and Fig. 1c shows the U_{vdW} variations as a function of P_{C60} for thirteen cases of Y_{disp}. In Fig. 2b, When $P_{C60} < -2$ nm, U_{vdW} decreases with increasing the Y_{disp} values. However, $P_{C60} > -2$ nm, and as Y_{disp} increases, U_{vdW} initially increases, then decreases, and finally re-increases, and this trend can be found in Fig. 1c. Such a result indicates that a C_{60} fullerene encapsulated in CNT might settle one of both sides with the lowest positions of U_{vdW} during the vibration of CNT. However, since these results were obtained from a static condition using the steepest descent method, these results could not entirely address the dynamics of the C_{60} encapsulated in CNT.

Therefore, we investigated the dynamics of the C_{60} encapsulated in CNT via MD simulations. We performed nine MD simula-

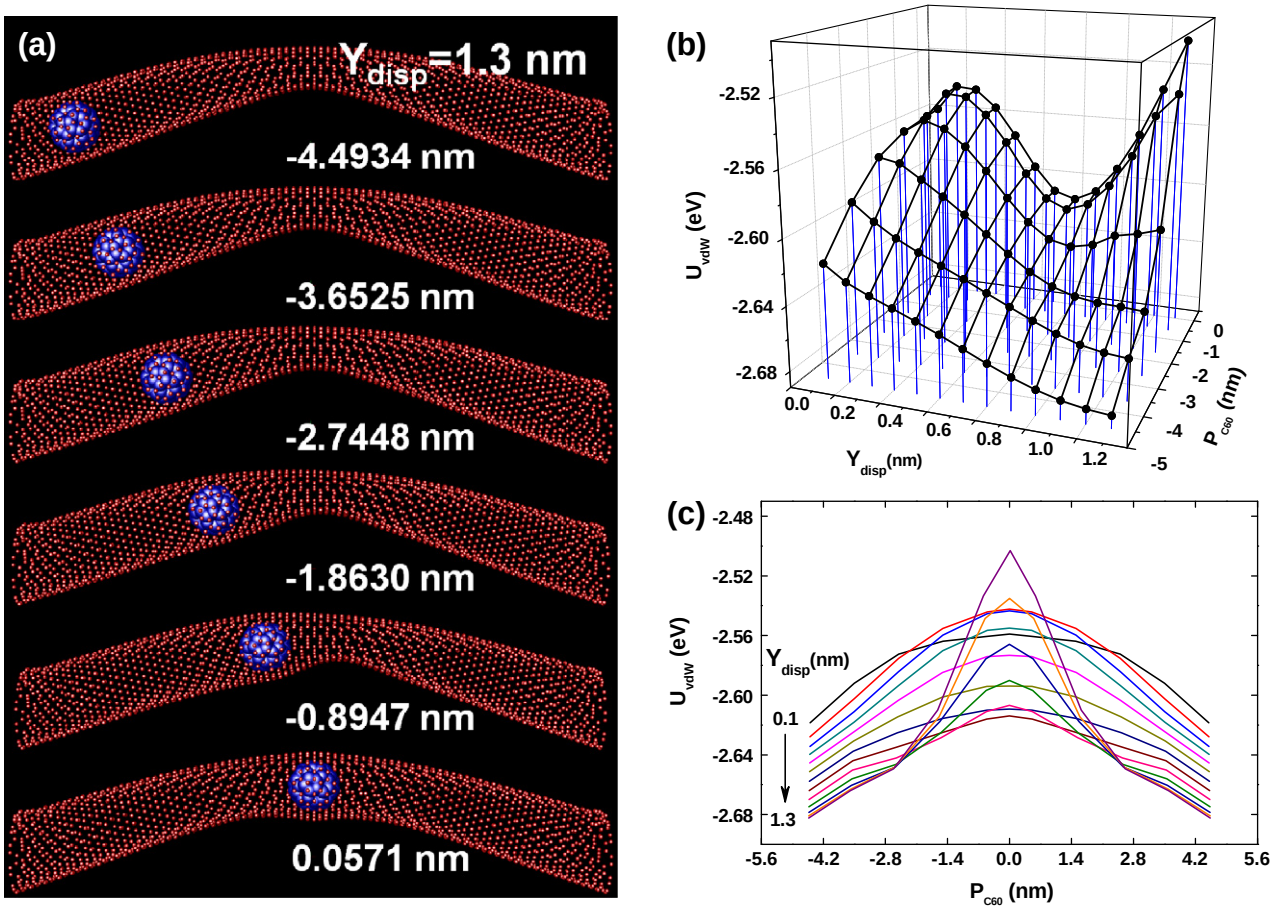

Fig. 1. (a) Six atomic configurations corresponding to six P_{C60} values for $Y_{disp} = 1.3$ nm. (b) A three-dimensional plot of U_{vdW} as functions of P_{C60} and Y_{disp}. (c) U_{vdW} variations as a function of P_{C60} for thirteen cases of Y_{disp}.

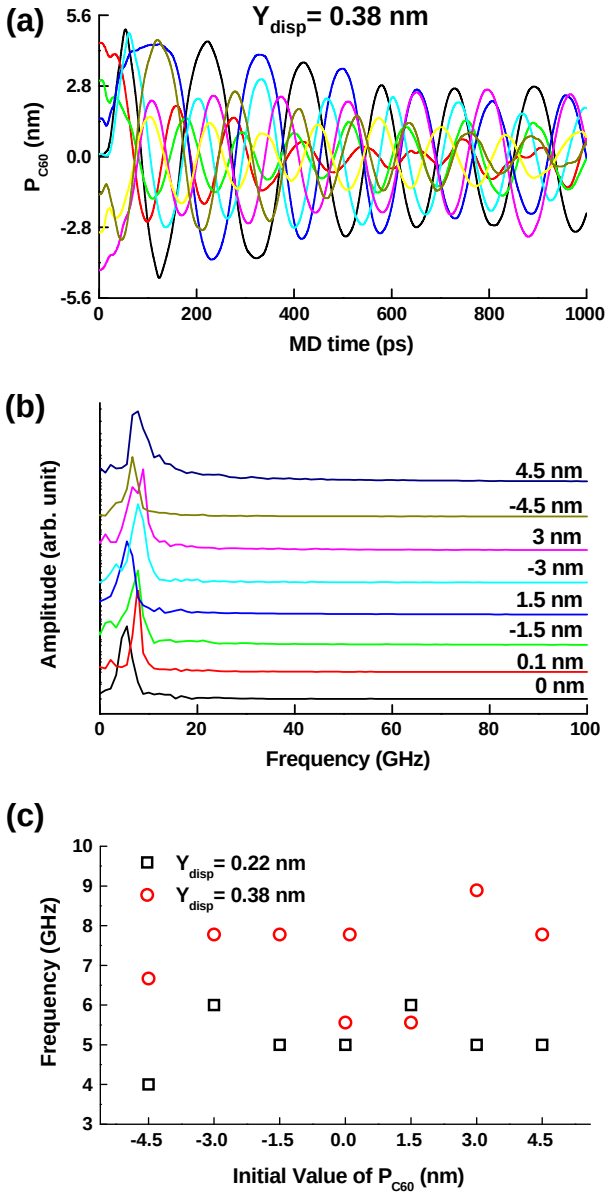

Fig. 2. (a) P_{C60} variations as a function of the MD time. (b) Amplitude spectra as a function of the frequency. (c) f_p as a function of the initial P_{C60} values for Y_{disp} = 0.22 and 0.38 nm.

tions for different P_{C60}s when Y_{disp} = 0.22 and 0.38 nm. For nine cases of the initial P_{C60}s with Y_{disp} = 0.38 nm, Fig. 2a and b show the variations of P_{C60} as a function of the MD time and the amplitude spectra as a function of frequency. The variations of P_{C60} in Fig. 2a were shown in damped oscillations. In Fig. 2b, one explicitly finds the resonance frequencies at the peaks for each spectrum. Thus, Fig. 2c shows the frequencies (f_p) at the amplitude peaks as a function of the initial P_{C60}s values for Y_{disp} = 0.22 and 0.38 nm. As shown in Fig. 2c, the Pearson correlation coefficient between f_p and the initial P_{C60} was 0.221, and this value implies that the initial P_{C60} value was not correlated with the values of f_p. The mean values of f_ps for Y_{disp} = 0.22 and 0.38 nm were 5.143 ± 0.261 and 7.778 ± 0.420 GHz, respectively. Such a result indicates that the values of f_p might be influenced by the value of Y_{disp}.

Hence, in order to investigate the f_p–Y_{disp} relationship, we performed MD simulations when the external forces with the resonance frequency were applied to C_{60}@CNT for Y_{disp} = 0 nm and P_{C60} = 0 nm. The amplitudes of the externally applied forces were changed from 0.0002 to 0.002 eV/Å. Fig. 3a shows the variations of P_{C60} as a function of the MD time of ten cases. The variations of P_{C60} were also found in damped oscillations as shown in Fig. 3a. We calculated the amplitude spectra as a function of the frequency as shown in Fig. 3b, and both f_p values and the mean values of Y_{disp} were then calculated. The labels in Fig. 3b indicate the mean Y_{disp} values. The relationship between f_p and the mean Y_{disp} was plotted in Fig. 3c. For Fig. 3c, the Pearson correlation coefficient between f_p and the mean Y_{disp} was 0.90173, and this value indicates that the f_p value was closely correlated with the value of the mean Y_{disp}. So, we obtained the fitting function of $y = 20.1x + 0.2064$.

As mentioned above, the variations of P_{C60} were also found in damped oscillations as shown in Figs. 2a and 3a. These figures show that the C_{60} fullerene was stabilized in the central region of the vibrating CNT along the tube axis. However, such a phenome-

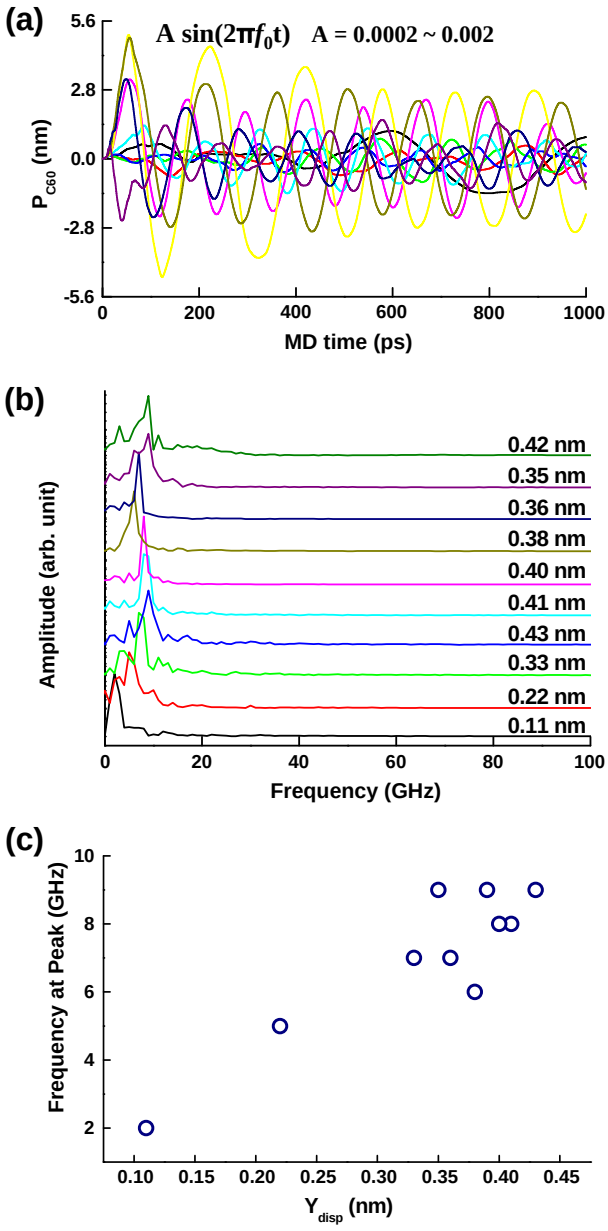

Fig. 3. (a) P_{C60} variations as a function of the MD time under different then external forces for P_{C60} = 0. (b) Spectra as a function of the frequency. The labels indicate the mean Y_{disp} values. (c) Relationship between f_p and the mean Y_{disp}.

non is not coincided with the discussion in Fig. 1, which the U_{vdW} is highest at the central position. Therefore, we calculated the acceleration values of the C_{60} fullerene exerted by vibrating CNT, using data obtained from the MD simulations. Fig. 4 shows the acceleration on the scale of nm/ps^2 as a function of P_{C60} when the initial P_{C60} = 0 nm and Y_{disp} = 0.38 nm. The acceleration values of the central regions were higher than those of the sides because the displacement of the center was highest; thus, the C_{60} fullerene moved toward the center position that had the highest acceleration force. As previously mentioned in the Section 1, the origin force, as a centrifugal force, due to such C_{60}-fullerene's oscillation occurring along the tube axis in the vibrating CNT is obviously different from the van der Waals interaction force that makes its oscillation a suction force at both edges, which has been extensively investigated using the fixed CNTs [25–31].

The encapsulated C_{60} fullerene oscillates centered on the position with the highest acceleration force is applicable as a data storage device. The movable C_{60} fullerene inside CNT can be applied to a nanotube-based data storage media by sensing the position of the C_{60} fullerene. When the CNT resonator is resonating at its fundamental frequency, its highest acceleration occurs at the center of the CNT resonator. Assuming that a C_{60} fullerene is encapsulated in the CNT resonator and is movable as a result of the acceleration force, the C_{60} fullerene finally settles around the center of the CNT resonator. When the CNT resonator is vibrating at its second-order resonance frequency, the highest accelerations occur at the two points that are 1/4 and 3/4 of the CNT length along the tube axis. So, for a CNT resonator encapsulating a C_{60} fullerene, the positions of the encapsulated C_{60} fullerene can be controlled by the order of the resonance frequency. Sensing the position of the C_{60} fullerene can be achieved by probing the electrical properties such as fullerene-shuttle memories [8–18].

The position probability distributions of the C_{60} fullerene during the vibration were calculated by the P_{C60} variations obtained from the MD simulations for 1, 100, and 200 K. Fig. 5a, c and e shows the P_{C60} variations with eight different initial positions for 1, 100, and 200 K, respectively. Fig. 5b, d and f shows the position probability distributions calculated using data after 600 ps for 1, 100, and 200 K, respectively, and such distributions are approximately fitted by Gaussian distribution functions. We can note that such a distribution is related to the acceleration force distribution as presented in Fig. 4. The probabilities at the center region are explicitly higher than those at both sides in all three cases. As the temperature increases, the peak values of the probability distributions decrease and their variations increase.

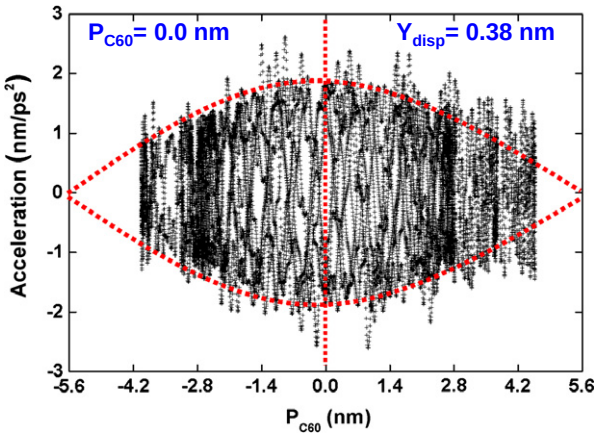

Fig. 4. Acceleration in the scale of nm/ps^2 as a function of P_{C60} when the initial P_{C60} = 0 nm and Y_{disp} = 0.38 nm.

The dynamics of a C_{60} fullerene encapsulated in the vibrating CNT are briefly summarized in Fig. 6a. The acceleration force (F_y) is highest at the center of the vibrating CNT, i.e., $z = 0$, and it decreases toward both clamps as shown in Fig. 4. In Fig. 6, the length of CNT is $2z_m$. The force (F_α) on the C_{60} fullerene, which makes its motion along the tube axis, can be expressed as

$$F_\alpha = F_y sin(\theta) + \xi, \tag{1}$$

where θ is the angle between the y-axis and the normal vector of the curved surface, as is shown in Fig. 6a, and ξ is a random force by van der Waals interaction. Here, we should note that even thought this van der Waals interaction force is statistically zero and can be negligible, it certainly affects the dynamics of the C_{60} fullerene. However, in this paper, this force effect was neglected because the oscillation of the C_{60} fullerene was obviously influenced on F_α. This angle θ as a function of time can be expressed as,

$$\theta = \theta_0 sin(2\pi f_0 t + \delta), \tag{2}$$

where f_0 and δ are the resonance frequency of the CNT resonator and the phase as the initial deformation, respectively. θ_0 is the maximum angle and is dependent on both the geometric parameters and mechanical properties such as Young's modulus, critical strength and Possion ratio; thus, it is expressed as:

$$\theta_0 = \gamma |y sin(\beta z)|, \tag{3}$$

where β is a constant, $-\pi/z_m$, and γ is an adjusted parameter for the mechanical properties. So, the time-dependent average force, $\widetilde{F}_\alpha(z)$, at z point can be obtained as

$$\widetilde{F}_\alpha(z) = \frac{1}{T}\int_t^{t+T} F_y(z) sin(\theta(t)) dt. \tag{4}$$

The equations above show that the effective force,$\widetilde{F}_\alpha$, increases with increasing y, which is closely related to Y_{disp}, and the oscillation frequency of the C_{60} fullerene linearly increases with increasing the acting force. Such a result is in excellent agreement with the results obtained from the MD simulations, according to which the f_p value was almost linearly proportional with the value of the mean Y_{disp} as shown in Fig. 3c. Assuming that the position (z) of the C_{60} fullerene be constant during a cycle, Fig. 6b shows the variations of $\widetilde{F}_\alpha$ values as a function of z for Y_{disp}, and $\widetilde{F}_\alpha$ can be expressed as an odd symmetric function, $\widetilde{F}_\alpha(-z/z_m)$, = $-\widetilde{F}_\alpha(z/z_m)$. As the Y_{disp} increases, the maximum value of $\widetilde{F}_\alpha$ increases. F_y is the highest at the center, $z = 0$, whereas $\widetilde{F}_\alpha$ is zero at $z = 0$. The positive $\widetilde{F}_\alpha$ is highest at $z/z_m = -0.5$, and the negative $\widetilde{F}_\alpha$ is lowest at $z/z_m = 0.5$, and such a dynamic is the origin of the oscillation motion; hence, the C_{60} fullerene can be oscillated by alternating $\widetilde{F}_\alpha$, and its motion can be repeatedly moved toward the center.

Since the MD simulations in this work did not include quantum effects, we could not provide electronic information on the migration of the C_{60} fullerene or the effects due to the quantum interference of the CNT resonator encapsulating the C_{60} fullerene. Therefore, the model used in this work cannot exactly describe the interaction and the dynamics. However, this work demonstrates the potential application of C_{60} fullerene encapsulated in CNTs as data storage media. Due to thermal energy dissipations, inter-energy exchanges, and inter-frictions can affect the motion of the C_{60} fullerene and the oscillation damping of the C_{60} fullerene in the vibrating CNT, there should be further work using MD simulations with different conditions including the van der Waals interactions.

In contrast to the empty fullerene cages, metal-containing endohedral fullerenes (metallofullerene or endo-fullerene) are known to have large electric dipole moments ranging between 3 and 4 Debye [39,40]. The metal embedded inside the fullerene has been found to depart from the center of the fullerene with

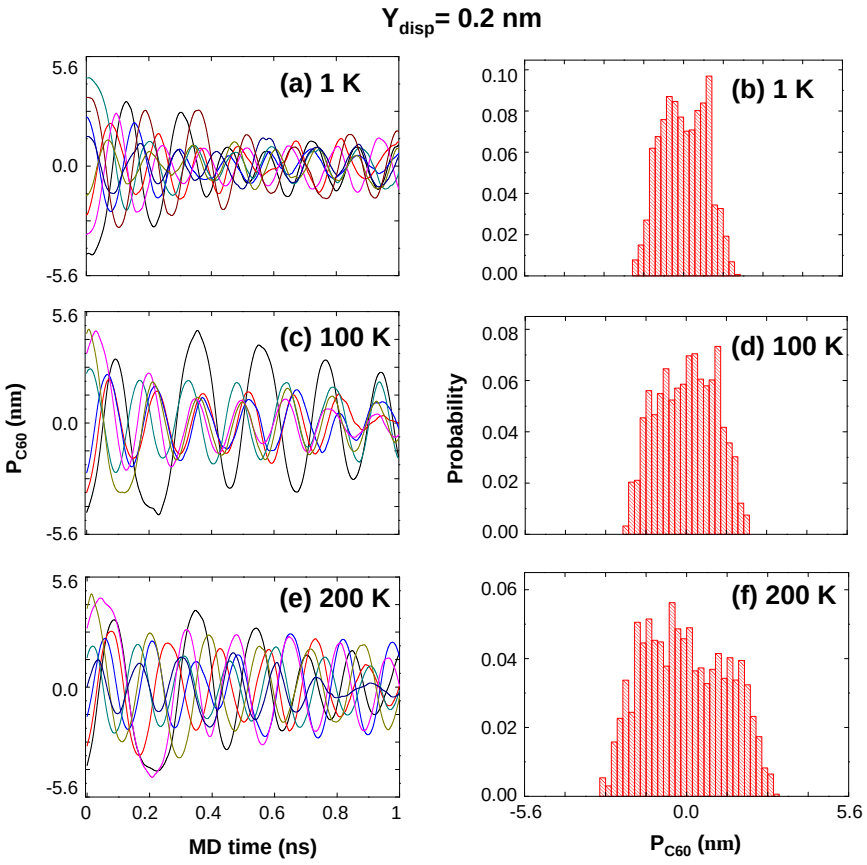

Fig. 5. P_{C60} variations with eight different initial positions for (a) 1 K, (c) 100 K, and (e) 200 K. Probability distributions calculated using data after 600 ps for (b) 1 K, (d) 100 K, and (f) 200 K.

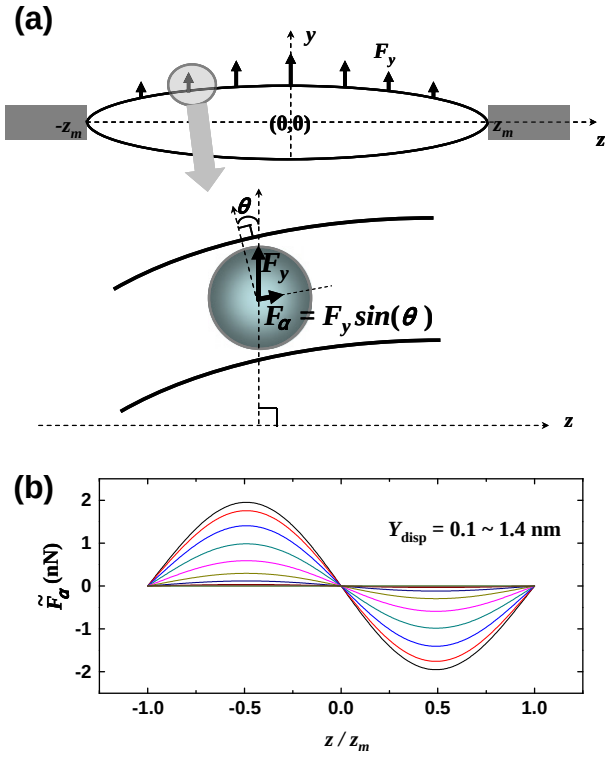

Fig. 6. (a) The dynamics of a C_{60} fullerene encapsulated in the vibrating CNT. (b) The variations of $\tilde{F}_\alpha$ values as a function of z/z_m for Y_{disp}.

charge transfer to the cage [41,42], and the intermolecular interactions in $M@C_n$, where M denotes the metal center and n denotes the total number of carbon atoms on the cage, are dominated by strong dipole interactions. Therefore, a multi-walled CNT encapsulating a charged endo-fullerene has potential applications as a CNT-based sensor that can be detected by external electromagnetic fields, and it can be used as a nano-electromagnetic source or as nano-memory. Therefore, there should be further investigations of multi-walled CNT resonators encapsulating various nanoclusters or endo-fullerenes.

4. Conclusions

The dynamics of a C_{60} fullerene encapsulated in a single-walled CNT resonator were investigated via classical molecular dynamics simulations. The C_{60} fullerene positions in a single-walled CNT resonator could be controlled by vibrating the resonator. The C_{60} fullerene approached the center of the single-walled CNT resonator where the exerted acceleration force was highest. C_{60}-fullerene's oscillations along the tube axis in a vibrating CNT were originated by centrifugal forces exerted at the central position of the CNT, and thus the property was very different from its oscillation in the fixed CNT. These properties suggest that a CNT resonator encapsulating a C_{60} fullerene has a potential application in a programmable multiple-position device controlled by the resonance frequency.

Acknowledgments

This research was supported by Basic Science Research Program through the National Research Foundation of Korea (NRF) funded

by the Ministry of Education, Science and Technology (MEST) (2010-0002299).

References

[1] H.G. Craighead, Science 290 (2000) 1532.
[2] S. Iijima, Nature 354 (1991) 56.
[3] V. Sazonova, Y. Yaish, H. Ustunel, D. Roundy, T.A. Arias, P.L. McEuen, Nature 431 (2004) 284.
[4] Q. Zheng, Q. Jiang, Phys. Rev. Lett. 88 (2002) 045503.
[5] D. Qian, G.J. Wagner, W.K. Liu, M.F. Yu, R.S. Ruoff, Appl. Mech. Rev. 55 (2002) 495.
[6] W.I.F. David, R.M. Ibberson, J.C. Mattewman, K. Prassides, T.J.S. Dennis, J.P. Hare, H.W. Kroto, R. Taylor, D.R.M. Walton, Nature 353 (1991) 147.
[7] M. Monthioux, Carbon 40 (2002) 1809.
[8] Y.K. Kwon, D. Tomanek, S. Iijima, Phys. Rev. Lett. 82 (1999) 1470.
[9] J.W. Kang, H.J. Hwang, J. Phys. Soc. Jpn. 73 (2004) 1077.
[10] J.W. Kang, H.J. Hwang, Physica E 23 (2004) 36.
[11] H.J. Hwang, K.R. Byun, J.Y. Lee, J.W. Kang, Curr. Appl. Phys. 5 (2005) 609.
[12] J. Lee, H. Kim, S.J. Kahng, G. Kim, Y.W. Son, J. Ihm, H. Kato, Z.W. Wang, T. Okazaki, H. Shinohara, Y. Kuk, Nature 415 (2002) 1005.
[13] J.W. Kang, H.J. Hwang, Physica E 27 (2005) 245.
[14] K.R. Byun, J.W. Kang, H.J. Hwang, Physica E 28 (2005) 50.
[15] H.J. Hwang, W.Y. Choi, J.W. Kang, Comput. Mater. Sci. 33 (2005) 317.
[16] W.Y. Choi, J.W. Kang, H.J. Hwang, Physica E 23 (2004) 135.
[17] J.W. Kang, J.H. Hwang, Mater. Sci. Eng. C 25 (2005) 843.
[18] J.W. Kang, H.J. Hwang, Carbon 42 (2004) 3018.
[19] J.W. Kang, Y.G. Choi, J.H. Lee, O.K. Kwon, H.J. Hwang, Mol. Simulat. 34 (2008) 829.
[20] Y. Dai, W. Guo, C. Li, C. Tang, J. Comput. Theor. Nanosci. 5 (2008) 1372.
[21] S.B. Legoas, V.R. Coluci, S.F. Braga, P.Z. Coura, S.O. Dantas, D.S. Galvão, Phys. Rev. Lett. 90 (2003) 055504.
[22] J.W. Kang, H.J. Hwang, Q. Jiang, J. Comput. Theor. Nanosci. 3 (2006) 880.
[23] Z. Qin, J. Zou, X.-Q. Feng, J. Comput. Theor. Nanosci. 5 (2008) 1403.
[24] J. Zhang, Y. Liu, M. Liu, W.M. Lau, J. Yang, J. Comput. Theor. Nanosci. 5 (2008) 1440.
[25] D. Qian, W.K. Liu, R.S. Ruoff, J. Phys. Chem. B 105 (2001) 10753.
[26] P. Liu, Y.W. Zhang, C. Lu, J. Appl. Phys. 97 (2005) 094313.
[27] X. Wang, H. Xin, J.N. Leonard, G. Chen, A.T. Chwang, Q. Jiang, J. Nanosci. Nanotechnol. 7 (2007) 1512.
[28] B.J. Cox, N. Thamwattana, J.M. Hill, J. Phys. A: Math. Theor. 40 (2007) 13197.
[29] B.J. Cox, N. Thamwattana, J.M. Hill, Proc. Roy. Soc. London A 463 (2007) 461.
[30] B.J. Cox, N. Thamwattana, J.M. Hill, Proc. Roy. Soc. London A 463 (2007) 477.
[31] B.J. Cox, N. Thamwattana, J.M. Hill, Proc. Roy. Soc. London A 646 (2008) 691.
[32] J. Tersoff, Phys. Rev. B 38 (1988) 9902.
[33] J. Tersoff, Phys. Rev. B 39 (1989) 5566.
[34] D.W. Brenner, Phys. Rev. B 42 (1990) 9458.
[35] H. Ulbricht, G. Moos, T. Hertel, Phys. Rev. Lett. 90 (2003) 095501.
[36] J.W. Kang, K.-S. Kim, H.J. Hwang, O.K. Kwon, Phys. Lett. A 374 (2010) 3658.
[37] J.W. Kang, C.S. Won, G.H. Ryu, Y.K. Choi, J. Nanosci. Nanotechnol. 9 (2009) 6943.
[38] J.H. Lee, K.-S. Kim, J.W. Kang, Comput. Mater. Sci. 48 (2010) 837.
[39] D.S. Bethune, R.D. Johnson, J.R. Salem, M.S. de Vries, C.S. Yannoni, Nature 366 (1993) 6451.
[40] K. Laasonen, W. Andreoni, M. Parrinello, Science 258 (1992) 1916.
[41] G.P. Li, R.F. Sabirianov, J. Lu, X.C. Zeng, W.N. Mei, J. Chem. Phys. 128 (2008) 074304.
[42] H. Shinohara, Rep. Prog. Phys. 63 (2000) 843.